Title: The *Phtheirospermum japonicum* isopentenyltransferase PjIPT1a regulates host cytokinin responses in *Arabidopsis*

Authors: Anne Greifenhagen[1], Isabell Braunstein[1], Jens Pfannstiel[2], Satoko Yoshida[3], Ken Shirasu[4,5], Andreas Schaller[1], Thomas Spallek[1*]

Affiliations: [1]Department of Plant Physiology and Biochemistry, University of Hohenheim, Stuttgart, 70599, Germany

[2]Core Facility Hohenheim, Mass Spectrometry Unit, University of Hohenheim, Stuttgart, 70599, Germany

[3]Division of Biological Science, Graduate School of Science and Technology, Nara Institute of Science and Technology, Ikoma, Nara, 630-0192, Japan

[4]RIKEN Center for Sustainable Resource Science, Yokohama, 230-0045, Japan

[5]Graduate School of Science, The University of Tokyo, Tokyo, 113-0033, Japan

Corresponding Author: Thomas Spallek, address as above, Phone: +49 711-459-22200, email: thomas.spallek@uni-hohenheim.de

ORCID ID:

Anne Greifenhagen (Orcid ID: 0000-0003-2979-3203)

Isabell Braunstein (N/A)

Jens Pfannstiel (Orcid ID: 0000-0002-7651-4302)

Satoko Yoshida (Orcid ID: 0000-0002-9999-7861)

Ken Shirasu (Orcid ID: 0000-0002-0349-3870)

Andreas Schaller (Orcid ID: 0000-0001-6872-9576)

Thomas Spallek (Orcid ID: 0000-0003-4425-1015)

Total word count: 2989

4 main figures (all colour), 4 supplemental figures, 3 supplemental tables

Summary

The hemiparasitic plant *Phtheirospermum japonicum* is a nutritional specialist that supplements its nutrient requirements by parasitizing other plants through haustoria. During parasitism, the *Phtheirospermum* haustorium transfers hypertrophy-inducing cytokinins (CKs) to the infected host root. The CK biosynthesis genes required for haustorium-derived CKs and the induction of hypertrophy are still unknown. We searched for haustorium-expressed isopentenyltransferases (IPTs) that catalyse the first step of CK biosynthesis, confirmed the specific expression by *in vivo* imaging of a promoter-reporter, and further analysed the subcellular localization, the enzymatic function, and contribution to inducing hypertrophy by studying CRISPR-Cas9 induced *Phtheirospermum* mutants. *PjIPT1a* was specifically expressed in intrusive cells of the haustorium close to the host vasculature. PjIPT1a and its closest homolog PjIPT1b located to the cytosol and showed isopentenyltransferases activity *in vitro* with differences in substrate specificity. Mutating *PjIPT1a* abolished parasite-induced CK responses in the host. A homolog of *PjIPT1a* with shared characteristics was also identified in the related weed *Striga hermonthica*. With *PjIPT1a* we identified a *bona fide* parasitism gene. We propose that *PjIPT1a* exemplifies how parasitism-related functions evolve through gene duplications and neofunctionalization.

Keywords

Cytokinin, parasite, haustorium, intrusive cells, hypertrophy, *Striga*, neofunctionalization

Introduction

Most parasitic species maintain some level of photosynthesis (hemiparasites), but access soil nutrients mainly by parasitizing other plants (Heide-Jorgensen, 2008; Brundrett & Tedersoo, 2018). The two main lineages of hemiparasitic plants, Santalales and the family of Orobanchaceae in the Lamiales account for more than 90% of all parasitic species (Nickrent, 2020). The greatest in-family diversity of hemiparasitic plants with varying degrees of host-dependency is found in the Orobanchaceae. In contrast to the agriculturally important weed *Striga hermonthica*, non-weedy species such as the model parasitic plant *Phtheirospermum japonicum* can propagate without being attached to a host (Clarke *et al.*, 2019).

Genetic adaptations to the parasitic lifestyle start to be revealed from the sequencing of transcriptomes and genomes of parasitic plants (Yang *et al.*, 2015; Vogel *et al.*, 2018; Sun *et al.*, 2018; Yoshida *et al.*, 2019). At the centre of these studies is the haustorium, a multi-cellular organ that facilitates infection and parasitism (Yoshida *et al.*, 2016; Kokla & Melnyk, 2018). Comparative transcriptomics in three Orobanchaceae species with varying degrees of host dependencies unearthed remarkable conservation of the transcriptional signatures during infection (Yang *et al.*, 2015). Further studies confirmed these tendencies also in other lineages (Vogel *et al.*, 2018; Sun *et al.*, 2018; Yoshida *et al.*, 2019). The term "core parasitism genes" describes the shared transcriptional behaviour of a group of homologous genes within a parasitic plant lineage (Yang *et al.*, 2015).

The concept of core parasitism genes may be extended to "core parasitism strategies". Strategies that are commonly observed during plant parasitism include the secretion of cell wall degrading enzymes and changes in hormone homeostasis (Brun *et al.*, 2020). For example, cytokinins are produced in haustoria of *Cuscuta japonicum*, *Santalum album* and *Phtheirospermum japonicum* (Zhang *et al.*, 2012; Furuhashi *et al.*, 2013; Spallek *et al.*, 2017). Transfer of cytokinin from the parasite to the host was demonstrated using *Arabidopsis* cytokinin biosynthesis mutants and transgenic *Phtheirospermum* roots that express a cytokinin-degrading enzyme (Spallek *et al.*, 2017). With prolonged cytokinin transfer, infected host tissue becomes hypertrophic, a symptom that is also induced by mistletoes, *Viscum album* (Loranthaceae in the order Santalales), and *Alectra vogelii* (Orobanchaceae) (Heide-Jorgensen, 2008).

86 Cytokinins are N^6-substituted adenine derivatives, of which isoprenoid cytokinins are most
87 prevalent in plants (Sakakibara, 2006). N^6-prenylation is catalysed by adenosine phosphate-
88 isopentenyltransferases (IPTs). Plant IPTs prefer dimethylallyl diphosphate (DMAPP) as
89 isoprenoid donor, and ATP and ADP (ATP/ADP-type IPTs) or tRNA (tRNA-type IPTs) as
90 isoprenoid acceptors (Kakimoto, 2001; Sakakibara, 2006). The agrobacterial IPTs, Tmr and
91 Tzs, prefer hydroxy-methylbutenyl diphosphate and AMP as substrates. Tmr and Tzs are
92 required for virulence and crown-gall formation (Akiyoshi *et al.*, 1984; Heinemeyer *et al.*,
93 1987). Overexpression of IPTs in *Arabidopsis* causes ectopic cytokinin responses (Kakimoto,
94 2001) indicating that IPTs catalyse the rate limiting step in cytokinin biosynthesis. In
95 *Arabidopsis*, the major route of cytokinin biosynthesis relies on ATP/ADP-type IPTs targeted
96 to plastids (AtIPT1, AtIPT4, AtIPT5, AtIPT8), to mitochondria (AtIPT7), or residing in the
97 cytosol and nucleus (AtIPT3, AtIPT4). tRNA-type IPTs (AtIPT2, AtIPT9) also localize to the
98 cytosol and nucleus (Kasahara *et al.*, 2004; Kieber & Schaller, 2014). The biological relevance
99 of different subcellular IPT locations is not known.
100
101 Here, we report the function of *Phtheirospermum PjIPT1a* as a *bona fide* core parasitism gene.
102 PjIPT1a is an unconventional plant isopentenyltransferase with parasitism-related features.
103 *PjIPT1a* uses AMP and ATP as prenyl acceptors and is located in the cytosol. It is expressed
104 in intrusive cells of the *Phtheirospermum* haustorium. Targeted gene-knockouts of *PjIPT1a* by
105 CRISPR/Cas9 suppressed parasite-induced cytokinin responses in the host. Similarities to
106 isopentenyltransferases from *Striga* suggest that hemiparasitic Orobanchaceae use common
107 strategies to manipulate host plants.

108 Materials and Methods

109 Plant growth conditions and transformation

110 *Phtheirospermum japonicum* (Okayama, wild-type) seeds were sterilized in 70% ethanol,
111 0.05% SDS for 10 minutes, and then washed with 98% ethanol. For transformation, plants were
112 grown on Gamborg B5 medium (Duchefa) supplemented with 1% sucrose at 25°C under long-
113 day conditions (16 h light). Seven-days-old *Phtheirospermum* seedlings were transformed with
114 *Agrobacterium rhizogenes* as previously described (Ishida *et al.*, 2011). Approximately four
115 weeks after transformation, *Phtheirospermum* seedlings with hairy roots were transferred to
116 0.8 % agar containing 300 µg/ml cefotaxime. Two days later, *Arabidopsis* Ws *pARR5:GFP*
117 seedlings grown for one week on MS (Duchefa) plates were aligned next to *Phtheirospermum*
118 hairy roots. One week later, infected plants were transferred to half-strength MS plates and
119 grown for additional 21 days. *Nicotiana benthamiana* plants were grown in soil under long-day
120 conditions at 25°C.

121

122 Phylogenetic analysis

123 IPT amino acid sequences were retrieved from public databases (NCBI), and by blast search
124 using IPT protein sequences as query against published genomes (Table **S1**). CLC Main
125 Workbench Version 8 was used to align protein sequences and to construct a phylogenetic tree
126 based on the UPGMA and Jake-Cantor algorithm with a bootstrap analysis of 1000 replicates.

127

128 Cloning, plasmid design and genotyping

129 We cloned the 2.6 kb upstream sequence of the *PjIPT1a* gene while removing an internal
130 Bpi1site into a GoldenGate vector that was then used to generate 3xVenus-NLS-based reporter
131 as previously described (Engler *et al.*, 2014; Cui *et al.*, 2016). Primer sequences are given in
132 Table **S2**. Open reading frames (ORFs) of *PjIPT1a* and *PjIPT1b* were first cloned into
133 pENTR/D-TOPO entry vector (Thermo Fisher Scientific) to generate GFP fusion constructs
134 using the pGWB5 binary vector (Nakagawa *et al.*, 2007). The putative chloroplast transit
135 peptide was cloned into pART7 using XhoI and ClaI (Thermo Fisher Scientific) and then into
136 pART27 (Gleave, 1992). An empty pGREEN vector was used to express *p35S:GFP* (Hellens
137 *et al.*, 2000). Goldengate-compatible vectors carrying *PjIPT1a*-specific gRNAs, *Cas9*, and the
138 transformation marker *p35S:DsRED* were assembled as previously described (Nekrasov *et al.*,
139 2013; Engler *et al.*, 2014). gRNAs were chosen based on their specificity to the intended target.
140 Individual hairy roots were genotyped by amplifying a 1651 bp long amplicon that contained
141 the 954 bp *PjIPT1a* gene. *PjIPT1a* alleles were cloned into pBluescript-II-SK(+) vectors for

142 sequencing. For expression in *E. coli*, ORFs of *PjIPT1a*, *PjIPT1b*, and *GST* were fused with a
143 C-terminal octa-His tag in the pET42 vector (Novagen).
144
145 Expression of proteins in *N. benthamiana* and *E. coli*
146 *Agrobacterium tumefaciens* GV3101 were infiltrated in a 10 mM MES (pH 5.6) and 10 mM
147 $MgCl_2$ buffer into approximately five-week-old *N. benthamiana* leaves, which were imaged
148 two days later. *PjIPT1a-His*, *PjIPT1b-His*, and *GST-His* in *E. coli* were expressed in BL21 RIL
149 cells and purified on NiNTA beads (Qiagen), then concentrated and desalted using Vivaspin
150 500 columns (Sartorius).
151
152 Microscopy
153 Hairy roots were imaged in water using a Zeiss Axio Image Z.1 fluorescence microscope.
154 *PjIPT1a* reporter activity was recorded with a Leica TCS SP5 II, the subcellular location of
155 fluorescent proteins with a Zeiss LSM 700 confocal microscope.
156
157 IPT-*in vitro* assays
158 IPT-*in vitro* assays were conducted as previously described (Brugière *et al.*, 2008). In brief, 8
159 µg of purified proteins were incubated with 1 mM DMAPP (Sigma) and 1 mM AMP or ATP
160 for two hours at 30°C in 12.5 mM Tris–HCl (pH 7.5), 37.5 mM KCl, 5 mM $MgCl_2$. The reaction
161 was stopped at 95°C and methanol precipitated. The supernatant was analysed by UHPLC-
162 MS/MS on a 1290 UHPLC system (Agilent) coupled to a Q-Exactive Plus Orbitrap mass
163 spectrometer equipped with a heated electrospray ionization (HESI) source (Thermo Fisher
164 Scientific). Analyte separation was achieved by a Phenomenex Luna Omega Polar C18 column.
165 Mobile phase A was 0.2% formic acid in water, and mobile phase B 0.2% formic acid in
166 acetonitrile. The HESI source was operated in positive ion mode, with a capillary voltage of
167 4.2 kV and an ion transfer capillary temperature of 360 °C. Mass spectra were acquired in MS
168 mode within the mass range of 150 to 800 m/z at a resolution of 70,000 FWHM using an
169 Automatic Gain Control (AGC) target of 3 × 106 of and 100 ms maximum ion injection time
170 (MIT). Data dependent MS/MS spectra in a mass range of 200 to 2000 m/z were generated for
171 the five most abundant precursor ions with a resolution of 17,500 FWHM using an AGC target
172 of 5 × 104, 64 ms MIT and a stepped collision energy of 15, 30 and 55. Xcalibur software
173 version 4.4.16.14 (Thermo Fisher Scientific) was used for instrument control and data
174 acquisition. Compound Discoverer software 3.2 (Thermo Fischer Scientific) was used for
175 analysing raw instrument data (.raw files) and peak area calculation.

Statistical analysis

The R packages Rmisc, readr, multcompView, ggplot2 and ggpubr were used for statistics (R Core Team, 2020).

180 Results

181 *PjIPT1a* is expressed in intrusive cells of *Phtheirospermum* haustoria

182 CK-biosynthesis is tightly regulated by environmental and developmental cues and restricted
183 to distinct tissues and cells. We thus reasoned that CK production in *Phtheirospermum*
184 haustoria requires the haustorium-specific expression of at least one *IPT* gene (Fig. **1a**). We
185 surveyed published *Phtheirospermum* transcriptomes for infection-specific expression of *IPTs*
186 and identified one, hereinafter referred to as *PjIPT1a*, that is upregulated in the course of
187 infection and shows 25-fold higher expression in intrusive cells relative to the rest of the
188 haustorium (Fig. **1b**)(Ogawa *et al.*, 2020)(Kurotani *et al.*, 2020). *PjIPT1a* expression increases
189 until day 3 of the infection and continues at a relatively high level for the later time points (Fig.
190 **1c**). This expression profile coincides with the induction of cytokinin response markers in
191 parasite and host, which become detectable from 3 - 4 dpi (days post-infection) and remain
192 visible until at least 30 dpi (Spallek *et al.*, 2017). Using a 2.6 kb *PjIPT1a* promoter fragment to
193 drive the expression of a *3xVenus-NLS* reporter, we confirmed the specific expression of the
194 *PjIPT1a* gene in intrusive cells of *Phtheirospermum* haustoria at 4 dpi of *Arabidopsis* roots (Fig.
195 **1d-f**). *PjIPT1a* is thus expressed in cells in close, likely direct, contact to the host vasculature
196 (Fig. **1g-i**).

197

198 *PjIPT1a* encodes a cytosolic IPT with homologs in *Striga hermonthica*

199 To validate the phylogenetic relationship of PjIPT1a to other *Phtheirospermum* IPTs, we
200 compared the amino acid sequences of PjIPTs to known plant IPTs and two agrobacterial IPTs,
201 Tzs and Tmr (Fig. **2a**). PjIPT1a clustered with other plant IPT1s, and was more similar to
202 proteins from the related parasitic species *Striga hermonthica* (Orobanchaceae, Lamiales) and
203 *Streptocarpus rexii* (Gesneriaceae, Lamiales) than to IPTs from more distantly related non-
204 parasitic species such as common hop (*Humulus lupulus*, Cannabaceae, Rosales) and
205 *Arabidopsis thaliana* (Brassicaceae, Brassicales). Two close homologs were detected for
206 PjIPT1a and its *Striga* ortholog ShIPT1a. Like *PjIPT1a*, only *ShIPT1a* is induced upon
207 infections but not *ShIPT1b* (Fig. **S1**).

208

209 Bioinformatics tools predict a chloroplast transit peptide (CTP) in the first 22 amino acids of
210 PjIPT1a; however, at a lower score compared to AtIPT1 and SrIPT1 (Table **S3**). Putative CTPs
211 of PjIPT1a and ShIPT1 are less than half as long as the CTPs predicted for AtIPT1 (71 amino
212 acids) and SrIPT1 (46 amino acids) (Table **S3**; Fig. **S2**). Therefore, we experimentally tested
213 subcellular localization of PjIPT1a and functionality of its CTP. A PjIPT1a-GFP fusion protein

214 transiently expressed in *N. benthamiana* located to cytosol and nucleus (Fig. **2a**), with no
215 apparent difference to the localization of free GFP (Fig. **2e**). Western-blots using anti-GFP
216 antibodies confirmed the integrity of the PjIPT1a-GFP full-length protein (Fig. **S3**). The data
217 thus suggest nuclear-cytoplasmic localization of PjIPT1a.
218
219 Nuclear-cytoplasmic localization is also observed for chloroplast-targeted AtIPT3, when it is
220 post-translationally modified by C-terminal farnesylation (Galichet *et al.*, 2008). To exclude
221 the possibility that post-translational modifications of PjIPT1a outside the putative CTP would
222 affect its localization, we analysed the subcellular targeting of super-folder GFP fused to the
223 predicted transit peptide (the first 22 amino acids) (Fig. **2b**). The localization of PjIPT1a(1-22)-
224 sfGFP was indistinguishable from PjIPT1a-GFP and free GFP (Fig. **1a,e**). The same nuclear-
225 cytoplasmic localization was also observed for PjIPT1b-GFP (Fig. **2d**). The putative CTP signal
226 in *Striga* ShIPT1a is even shorter (11 amino acids) than the apparently non-functional CTP of
227 PjIPT1a (Fig. **S2**; Table **S3**), while no CTP was predicted for ShIPT1b. Therefore, we assume
228 a similar subcellular localization pattern of the homologous ShIPT1a and ShIPT1b proteins.
229
230 PjIPT1a drives CKs responses in host plants
231 Haustorium-derived CKs induce hypertrophy of the host root and can be visualized by a host-
232 expressed cytokinin reporter (*pARR5:GFP*)(Spallek *et al.*, 2017). To address a role for *PjIPT1a*
233 in the production of haustorium-derived CKs, we generated transgenic *Phtheirospermum* roots
234 (hairy root, HR) that expressed the *Cas9* gene together with two *PjIPTa*-specific gRNAs (Fig.
235 **3b**). The construct also contained *p35S:dsRED* as a fluorescent marker for identification of
236 transformed roots. HR transformed with *p35S:dsRED* alone served as controls. In contrast to
237 control HRs that triggered *pARR5:GFP* expression and hypertrophic growth in infected
238 *Arabidopsis* roots, neither *pARR5:GFP* expression nor hypertrophic growth were observed
239 after infection with HRs containing the *Cas9/PjIPT1a-gRNA*s cassette (Fig. **3a**). While the
240 *PjIPT1a* locus was successfully PCR-amplified from control HR (Fig. **3c**), smaller bands were
241 observed for HRs containing the *Cas9* gene (Fig. **3c**) resulting from Cas9-induced deletions
242 ranging from single-nucleotides to 1100 bp (Fig. **3d**). Despite low abundance, we also identified
243 one additional allele that carried a 40 bp deletion in the *PjIPT1a* gene for the hairy root HR3.
244 With the more abundant alleles with larger deletions (893 bp and 1110 bp), this third allele
245 revealed a chimeric pattern of *Cas9*-induced mutations in *Phtheirospermum* hairy roots. The
246 presence of Cas9-induced deletions in *PjIPT1a* correlated perfectly with the absence of a

247 *Phtheirospermum*-induced cytokinin response in *Arabidopsis*. We therefore conclude that
248 *PjIPT1a* is an essential component in the CK transfer from parasite to host.
249
250 PjIPT1a and PjIPT1b differ in isopentenyltransferase activity
251 PjIPT1a and ShIPT1a share a unique triple-proline motif close to the nucleotide-binding site
252 that we only found in IPTa isoforms of parasitic Orobanchaceae species (Fig. **S4**). This raised
253 questions regarding their enzymatic activity. We purified His-tagged PjIPT1a and PjIPT1b
254 from *E. coli* and assayed for isoprenylation of AMP and ATP with DMAPP as the isoprenyl
255 donor and His-tagged GST as negative control (Fig. **4**). When AMP was used as substrate, the
256 total amount of isoprenylated products were similar (factor of 1.3) for PjIPT1a-His and PjIPTb-
257 His (Fig. **4a**). However, with ATP as substrate, the total amount of isoprenylated products was
258 about five times higher for PjIPT1b-His compared to PjIPT1a-His, indicating higher selectivity
259 for ATP over AMP (Fig. **4b**).

260 Discussion

261 Here, we studied parasite-induced CK responses in host plants as an example of a
262 neofunctionalized gene function in the Orobanchaceae species *Phtheirospermum japonicum*
263 and *Striga hermonthica*. We found one IPT gene, *PjIPT1a*, to be expressed in *Phtheirospermum*
264 haustoria. Reporter gene analysis revealed spatially restricted activity of the *PjIPT1a* promotor
265 in intrusive cells that are in contact with the host vasculature (Fig. **1g-i**). The proximity to the
266 host vasculature is likely sufficient to transfer cytokinins to the host and to trigger CK responses
267 above the haustorium attachment site (Spíchal, 2012). The parasitic tree *Santalum album* also
268 expresses an IPT1 homolog at a similar stage of infections; however, the exact location of
269 *SaIPT1* expressing cells is not known (Zhang *et al.*, 2015).

270

271 Unlike in *Santalum album* and many other parasitic plants that are not amenable to reverse
272 genetic manipulation, we were able to use CRISPR/Cas9-based loss-of-function analysis to
273 demonstrate that *PjIPT1a* adopted new parasitism-related functions in *Phtheirospermum*.
274 While RNAi-based knock-down approaches have largely been replaced by the CRISPR/Cas9
275 technology, RNAi remained, until now, the only strategy to study parasitic plant genes
276 (Bandaranayake *et al.*, 2010; Alakonya *et al.*, 2012; Wakatake *et al.*, 2020). Here, we report the
277 first successful application of the CRISPR/Cas9 technology for studying loss-of-function
278 phenotypes in parasitic plants. CRISPR/Cas9 efficiently introduced deletions in *PjIPT1a*
279 resulting in the loss of up to 98% of the coding sequence, or in the disruption of its open reading
280 frame. In individual hairy roots, we found more than one, in one instance more than two,
281 mutated alleles of *PjIPT1a*, a result of the occasionally chimeric nature of *Agrobacterium*
282 *rhizogenes*-induced hairy roots (Wakatake *et al.*, 2018). All *Phtheirospermum* roots with non-
283 functional *PjIPT1a* genes failed to induce host CK responses (Fig. **3b,c**), showing that *PjIPT1a*
284 is indeed a *bona fide* parasitism gene with a specific parasitism-related physiological function.

285

286 As previously proposed for other parasitism genes in the Orobanchaceae, our phylogenetic
287 analysis of *IPTs* showed that the duplication event producing *PjIPT1a/ShIPT1a* and
288 *PjIPT1b/ShIPT1b* occurred in a common non-parasitic ancestor of *P. japonicum* and *S.*
289 *hermonthica* (Yang *et al.*, 2015). Surprisingly, PjIPT1a and ShIPT1a, which adopted a new
290 function as parasitism genes, are more similar to SrIPT1 from *Streptocarpus rexii* than PjIPT1b
291 and ShIPT1b (Fig. **2a**). The high similarity between parasitism-related and conventional IPTs
292 suggests that neofunctionalization of *PjIPT1a* mainly occurred at the level of its expression
293 profile. Enzymatic constraints may have limited divergence of the gene body and the enzymatic

294 functions of PjIPT1a and b are indeed comparable. However, preference for ATP was reduced
295 in PjIPT1a; its preference for the energetically less costly AMP as isopentenyl donor may
296 reflect an adaptation to the resource-limited parasitic lifestyle that is induced under nutrient-
297 deficient conditions (Spallek *et al.*, 2017). A notable exception to the similarity of PjIPT1a and
298 ShIPT1a to SrIPT1 is a characteristic triple-proline-motif that is only found in parasitism-
299 related IPTs (Fig. **S4**).
300
301 Another unexpected feature of PjIPT1a is its nuclear-cytoplasmic localization (Fig. **2b,c**),
302 which it shares with PjIPT1b (Fig. **2d**) and likely also with ShIPT1a and ShIPT1b (Table **S1**).
303 *Arabidopsis* AtIPT1 and AtIPT3 feature functional N-terminal CTPs (Kasahara *et al.*, 2004).
304 However, while AtIPT1 is located in plastids, AtIPT3 is dually targeted, either to the chloroplast,
305 or to the nucleus/cytoplasm in a farnesylation-dependent manner (Galichet *et al.*, 2008). We
306 can exclude a similar mechanism for PjIPT1a, as its predicted CTP appeared to be non-
307 functional, as it was insufficient for targeting GFP to plastids (Fig. **2c**). The relevance of the
308 nuclear-cytoplasmic localization is not clear, but given that it is shared between IPTs that are
309 up-regulated during infection and other that are not, a functional link to parasitism seems
310 unlikely.
311
312 In conclusion, we identified *PjIPT1a* as a *bona fide* parasitism gene that originated from a non-
313 parasitic ancestral gene through gene duplication followed by neofunctionalization. Targeted
314 knock-out of *PjIPT1a* showed its essential role for *Phtheirospermum*-induced CK-responses in
315 the host. PjIPT1a has homologs in other parasitic plants. Targeting of neofunctionalized
316 parasitism genes may allow for specific control of parasitic weeds leaving host plants unharmed.

Acknowledgements

This work supported by the German Research Foundation (DFG, 424122841) to T.S and MEXT KAKENHI JP20H05909 to S.Y. and K.S. The authors thank Ursula Glück-Behrens and Ute Bertsche for technical support.

Author Contribution

T.S., A.S., and K.S supervised the research. A.G. and I.B. analysed the subcellular location of proteins, purified IPTs from *E. coli* and conducted the *in vitro* assays. J.P. measured the IPT *in vitro* assays compounds by HPLC-MS/MS. T.S. performed the remaining experiments. A.S., P.S., and T.S. analysed data. Y.S. and K.S. provided crucial non-published data. T.S. and A.S. wrote the paper.

References

Akiyoshi DE, Klee H, Amasino RM, Nester EW, Gordon MP. 1984. T-DNA of *Agrobacterium tumefaciens* encodes an enzyme of cytokinin biosynthesis. *Proceedings of the National Academy of Sciences*, *USA* **81**: 5994–5998.

Alakonya A, Kumar R, Koenig D, Kimura S, Townsley B, Runo S, Garces HM, Kang J, Yanez A, David-Schwartz R, *et al.* 2012. Interspecific RNA interference of *SHOOT MERISTEMLESS*-like disrupts *Cuscuta pentagona* plant parasitism. *Plant Cell* **24:** 3153–3166.

Bandaranayake PCG, Filappova T, Tomilov A, Tomilova NB, Jamison-McClung D, Ngo Q, Inoue K, Yoder JI. 2010. A single-electron reducing quinone oxidoreductase is necessary to induce haustorium development in the root parasitic plant *Triphysaria*. *Plant Cell* **22:** 1404–1419.

Bardgett RD, Smith RS, Shiel RS, Peacock S, Simkin JM, Quirk H, Hobbs PJ. 2006. Parasitic plants indirectly regulate below-ground properties in grassland ecosystems. *Nature* **439:** 969–972.

Brugière N, Humbert S, Rizzo N, Bohn J, Habben JE. 2008. A member of the maize isopentenyl transferase gene family, *Zea mays isopentenyl transferase 2* (*ZmIPT2*), encodes a cytokinin biosynthetic enzyme expressed during kernel development. *Plant Molecular Biology* **67:** 215–229.

Brun G, Spallek T, Simier P, Delavault P. 2020. Molecular actors of seed germination and haustoriogenesis in parasitic weeds. *Plant Physiology* **185:** 1270-1281.

350 **Brundrett MC, Tedersoo L. 2018.** Evolutionary history of mycorrhizal symbioses and global
351 host plant diversity. *New Phytologist* **220:** 1108–1115.
352 **Clarke CR, Timko MP, Yoder JI, Axtell MJ, Westwood JH. 2019.** Molecular dialog
353 between parasitic plants and their hosts. *Annual Review of Phytopathology* **57:** 279–299.
354 **Cui S, Wakatake T, Hashimoto K, Saucet SB, Toyooka K, Yoshida S, Shirasu K. 2016.**
355 Haustorial hairs are specialized root hairs that support parasitism in the facultative parasitic
356 plant *Phtheirospermum japonicum*. *Plant Physiology* **170:** 1492–1503.
357 **Engler C, Youles M, Gruetzner R, Ehnert TM, Werner S, Jones JDG, Patron NJ,**
358 **Marillonnet S. 2014.** A golden gate modular cloning toolbox for plants. *ACS Synthetic Biology*
359 **3:** 839–843.
360 **Furuhashi T, Kojima M, Sakakibara H, Fukushima A, Hirai MY, Furuhashi K. 2013.**
361 Morphological and plant hormonal changes during parasitization by *Cuscuta japonica* on
362 *Momordica charantia*. *Journal of Plant Interactions* **9:** 220–232.
363 **Galichet A, Hoyerová K, Kamínek M, Gruissem W. 2008.** Farnesylation directs AtIPT3
364 subcellular localization and modulates cytokinin biosynthesis in *Arabidopsis*. *Plant Physiology*
365 **146:** 1155–1164.
366 **Gleave AP. 1992.** A versatile binary vector system with a T-DNA organisational structure
367 conducive to efficient integration of cloned DNA into the plant genome. *Plant Molecular*
368 *Biology* **20:** 1203–1207.
369 **Heide-Jorgensen H. 2008.** *Parasitic Flowering Plants.* Leiden: Brill Academic Publishers.
370 **Heinemeyer W, Buchmann I, Tonge DW, Windass JD, Alt-Moerbe J, Weiler EW, Botz T,**
371 **Schröder J. 1987.** Two *Agrobacterium tumefaciens* genes for cytokinin biosynthesis: Ti
372 plasmid-coded isopentenyltransferases adapted for function in prokaryotic or eukaryotic cells.
373 *Molecular and General Genetics* **210:** 156–164.
374 **Hellens RP, Edwards E a, Leyland NR, Bean S, Mullineaux PM. 2000.** pGreen: a versatile
375 and flexible binary Ti vector for *Agrobacterium*-mediated plant transformation. *Plant*
376 *Molecular Biology* **42:** 819–832.
377 **Ishida JK, Yoshida S, Ito M, Namba S, Shirasu K. 2011.** *Agrobacterium rhizogenes*-
378 mediated transformation of the parasitic plant *Phtheirospermum japonicum*. *PloS one* **6:**
379 e25802.
380 **Kakimoto T. 2001.** Identification of plant cytokinin biosynthetic enzymes as dimethylallyl
381 diphosphate:ATP/ADP isopentenyltransferases. *Plant and Cell Physiology* **42:** 677–685.

382 **Kasahara H, Takei K, Ueda N, Hishiyama S, Yamaya T, Kamiya Y, Yamaguchi S,**
383 **Sakakibara H. 2004.** Distinct isoprenoid origins of cis- and trans-zeatin biosyntheses in
384 *Arabidopsis*. *Journal of Biological Chemistry* **279:** 14049–14054.
385 **Kieber JJ, Schaller GE. 2014.** Cytokinins. *The Arabidopsis Book* **12:** e0168.
386 **Kokla A, Melnyk CW. 2018.** Developing a thief: Haustoria formation in parasitic plants.
387 *Developmental Biology* **442:** 53–59.
388 **Kurotani K, Wakatake T, Ichihashi Y, Okayasu K, Sawai Y, Ogawa S, Suzuki T, Shirasu**
389 **K, Notaguchi M. 2020.** Host-parasite tissue adhesion by a secreted type of β-1,4-glucanase in
390 the parasitic plant *Phtheirospermum japonicum*. *Communications Biology* **3:** 407.
391 **Miyawaki K, Matsumoto-Kitano M, Kakimoto T. 2004.** Expression of cytokinin
392 biosynthetic isopentenyltransferase genes in *Arabidopsis*: tissue specificity and regulation by
393 auxin, cytokinin, and nitrate. *The Plant Journal* **37:** 128–138.
394 **Nakagawa T, Kurose T, Hino T, Tanaka K, Kawamukai M, Niwa Y, Toyooka K,**
395 **Matsuoka K, Jinbo T, Kimura T. 2007.** Development of series of gateway binary vectors,
396 pGWBs, for realizing efficient construction of fusion genes for plant transformation. *Journal*
397 *of Bioscience and Bioengineering* **104:** 34–41.
398 **Nekrasov V, Staskawicz B, Weigel D, Jones JDG, Kamoun S. 2013.** Targeted mutagenesis
399 in the model plant *Nicotiana benthamiana* using Cas9 RNA-guided endonuclease. *Nature*
400 *Biotechnology* **31:** 691–693.
401 **Nickrent DL. 2020.** Parasitic angiosperms: How often and how many? *TAXON* **69:** 5–27.
402 **Ogawa S, Wakatake T, Spallek T, Ishida JK, Sano R, Kurata T, Demura T, Yoshida S,**
403 **Ichihashi Y, Schaller A, Shirasu K., 2020.** Subtilase activity in intrusive cells mediates
404 haustorium maturation in parasitic plants. *Plant Physiology* **185:** 1381-1394.
405 **R Core Team 2020.** R: A language and environment for statistical computing. R Foundation
406 for Statistical Computing, Vienna, Austria.
407 **Sakakibara H. 2006.** Cytokinins: activity, biosynthesis, and translocation. *Annual Review of*
408 *Plant Biology* **57:** 431–49.
409 **Spallek T, Melnyk CW, Wakatake T, Zhang J, Sakamoto Y, Kiba T, Yoshida S,**
410 **Matsunaga S, Sakakibara H, Shirasu K. 2017.** Interspecies hormonal control of host root
411 morphology by parasitic plants. *Proceedings of the National Academy of Sciences*, *USA* **114:**
412 5283–5288.
413 **Spíchal L. 2012.** Cytokinins - Recent news and views of evolutionally old molecules.
414 *Functional Plant Biology* **39:** 267–284.

415 **Sun G, Xu Y, Liu H, Sun T, Zhang J, Hettenhausen C, Shen G, Qi J, Qin Y, Li J, et al.**
416 **2018.** Large-scale gene losses underlie the genome evolution of parasitic plant *Cuscuta*
417 *australis*. *Nature Communications* **9:** 2683.
418 **Vogel A, Schwacke R, Denton AK, Fischer K, Bolger A, Marie E, Gundlach H, Mayer**
419 **KFX, Weiss-Schneeweiss H, Eva M, et al. 2018.** Footprints of parasitism in the genome of
420 the parasitic flowering plant *Cuscuta campestris*. *Nature Communications* **9:** 2515.
421 **Wakatake T, Ogawa S, Yoshida S, Shirasu K. 2020.** An auxin transport network underlies
422 xylem bridge formation between the hemi-parasitic plant *Phtheirospermum japonicum* and host
423 *Arabidopsis*. *Development* **147:** dev187781.
424 **Wakatake T, Yoshida S, Shirasu K. 2018.** Induced cell fate transitions at multiple cell layers
425 configure haustorium development in parasitic plants. *Development* **145:** dev164848.
426 **Yang Z, Wafula EK, Honaas LA, Zhang H, Das M, Fernandez-Aparicio M, Huang K,**
427 **Bandaranayake PCG, Wu B, Der JP, et al. 2015.** Comparative transcriptome analyses reveal
428 core parasitism genes and suggest gene duplication and repurposing as sources of structural
429 novelty. *Molecular Biology and Evolution* **32:** 767–790.
430 **Yoshida S, Cui S, Ichihashi Y, Shirasu K. 2016.** The Haustorium, a specialized invasive
431 organ in parasitic plants. *Annual Review of Plant Biology* **67:** 643–667.
432 **Yoshida S, Kim S, Wafula EK, Tanskanen J, Kim Y-M, Honaas L, Yang Z, Spallek T,**
433 **Conn CE, Ichihashi Y, et al. 2019.** Genome sequence of *Striga asiatica* provides insight into
434 the evolution of plant parasitism. *Current Biology* **29:** 3041-3052.
435 **Zhang X, Berkowitz O, Teixeira da Silva JA, Zhang M, Ma G, Whelan J, Duan J. 2015.**
436 RNA-Seq analysis identifies key genes associated with haustorial development in the root
437 hemiparasite *Santalum album*. *Frontiers in Plant Science* **6:** 661.
438 **Zhang X, Teixeira da Silva JA, Duan J, Deng R, Xu X, Ma G. 2012.** Endogenous hormone
439 levels and anatomical characters of haustoria in *Santalum album* L. seedlings before and after
440 attachment to the host. *Journal of Plant Physiology* **169:** 859–866.

441 Figure legends

442

443 **Figure 1:** ***PjIPT1a*** **is specifically expressed in intrusive cells.** (a) Prenylation of
444 adenosine-tri-, -di- and -mono-phosphates (ATP, ADP, AMP) by isopentenyltransferase (IPT)
445 with di-methylallyl pyrophosphate (DMAPP) to isopentyl-ribosides (IPR) is the first step of
446 cytokinin (CK) biosynthesis. (b) RNA-Sequencing data showing increased expression of
447 *PjIPT1a* in intrusive cells of *Phtheirospermum* (Pj) haustoria five days-post infection (dpi) of
448 rice roots (*Oryza sativa*, *Os*), and (c) upregulation of *PjIPT1a* expression during infection of
449 Arabidopsis (*At*) roots with a maximum of 61 CPM (counts per million mapped reads) at 3 dpi.
450 (d - i) Confocal images show a *Phtheirospermum* haustorium expressing
451 *pIPT1:PjIPT1:3xVenus-NLS* during infection of Arabidopsis (At) at 4 dpi. Merged yellow
452 channel for Venus detection and bright-field is depicted in (d), individual Venus and bright-
453 field channels in (e) and (f), respectively. Zoomed-in scans shown in g - i correspond to the
454 region marked by dotted lines in (d – f). Intrusive cells are indicated with white arrows. Scale
455 bars = 100 µm.

456

457 **Figure 2:** ***PjIPT1a*** **and its closest homolog are nuclear-cytoplasmic IPTs** Phylogenetic
458 analysis (UPGMA) based on the amino acid sequences of prokaryotic (*Agrobacterium*) and
459 plant IPTs positions IPT1a within a cluster of plant IPT1s and closest to the *Striga* ShIPT1a
460 protein. Bootstrap values are shown as percentage of 1000 repetitions. (b) PjIPT1a and PjIPT1b
461 (c) located in the cytoplasm and nucleus when expressed in *N. benthamiana*. The subcellular
462 localization pattern of the full-length PjIPT1a-GFP and PjIPT1b-GFP fusions matched the
463 pattern observed for PjIPTa$^{(1-22)}$-sfGFP (d) and free GFP (e). Scale bar = 50 µm.

464

465 **Figure 3:** ***PjIPT1a*** **drives host CK responses at the haustorium.** (a) Control (con.)
466 haustoria of hairy roots without the *Cas9/PjIPT1a-gRNA*s cassette (HR1, HR2) induced the
467 expression of host CK-response reporter *pARR5:GFP* and hypertrophic growth (arrows)
468 whereas haustoria with the *Cas9/PjIPT1a-gRNA*s cassette (HR3-4) did not. Images were taken
469 at 28 dpi, scale bars = 100 µm (b) Schematic representation of the *PjIPT1a* gene flanked by the
470 5' and 3' extension that were amplified in (c). Red colour highlights the target sequences of the
471 guide RNAs (c) PCR amplicons of the *PjIPT1a* and the *CAS9* genes in Phtheirospermum hairy
472 roots were sequenced to determine *CAS9-induced mutation (red)* as shown in (d). PAM
473 sequences are depicted in orange, the start codon in bold font.

474

475 **Figure 4: PjIPT1a and PjIPT1b are isopentyltransferases.** Plots show average +/- SD
476 (n = 3 – 6) peak areas of extracted-ion chromatograms of individual and cumulative (sum)
477 quantifications of isoprenylated derivatives that were detected in reaction mixtures containing
478 DMAPP, equal amounts of *E. coli* purified GST-His, PjIPT1b-His or PjIPT1b-His, and (a)
479 AMP or (b) ATP as isoprenoid acceptors. Different lower-case letters indicate significant
480 differences according to Tukey HSD with 95% confidence levels.

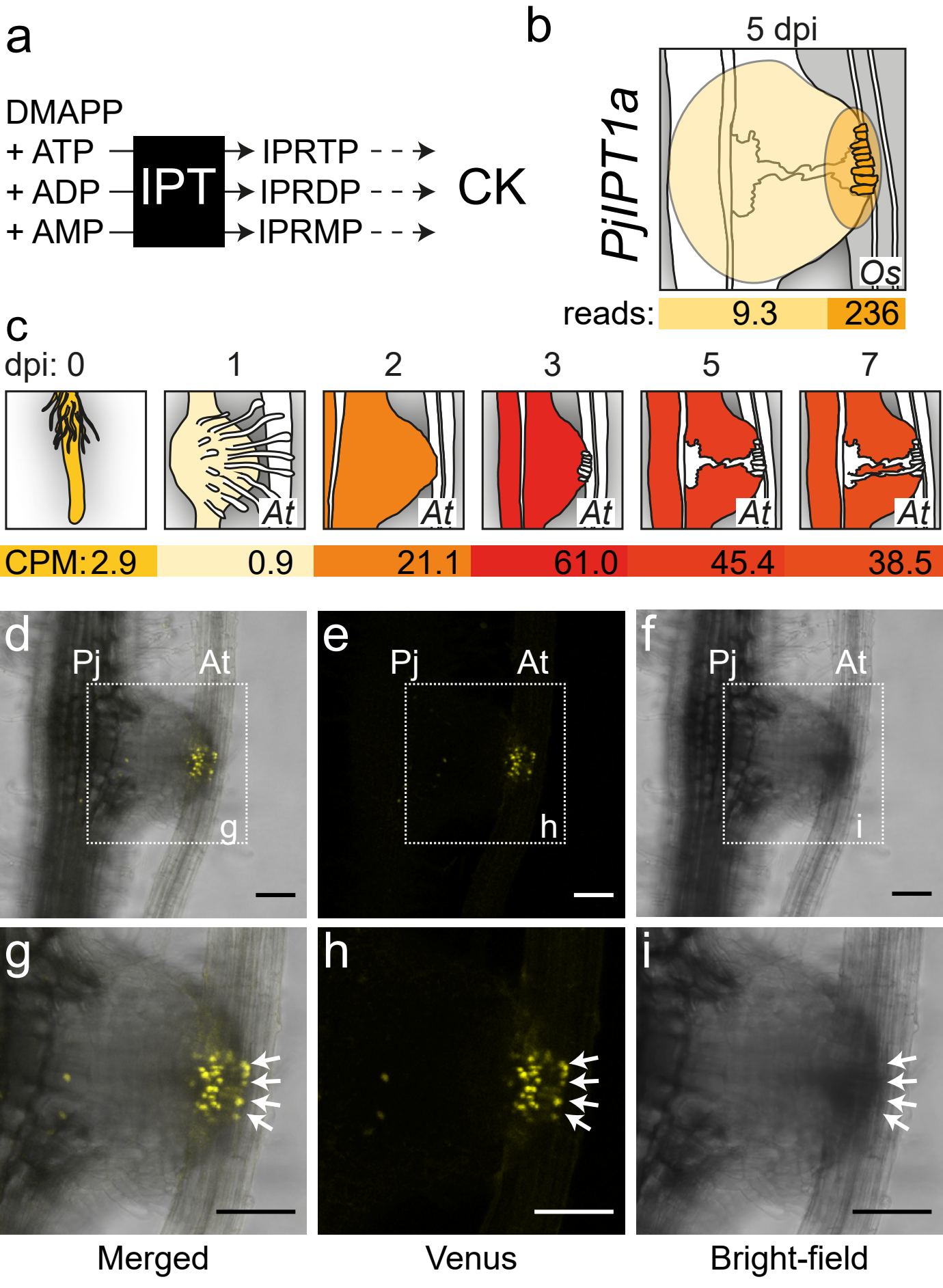
a
DMAPP
+ ATP
+ ADP
+ AMP
IPT
IPRTP
IPRDP
IPRMP
CK
b
5 dpi
PjIPT1a
Os
reads:
9.3
236
c
dpi: 0
1
2
3
5
7
At
CPM:2.9
0.9
21.1
61.0
45.4
38.5
d
e
f
Pj
At
g
h
i
Merged
Venus
Bright-field

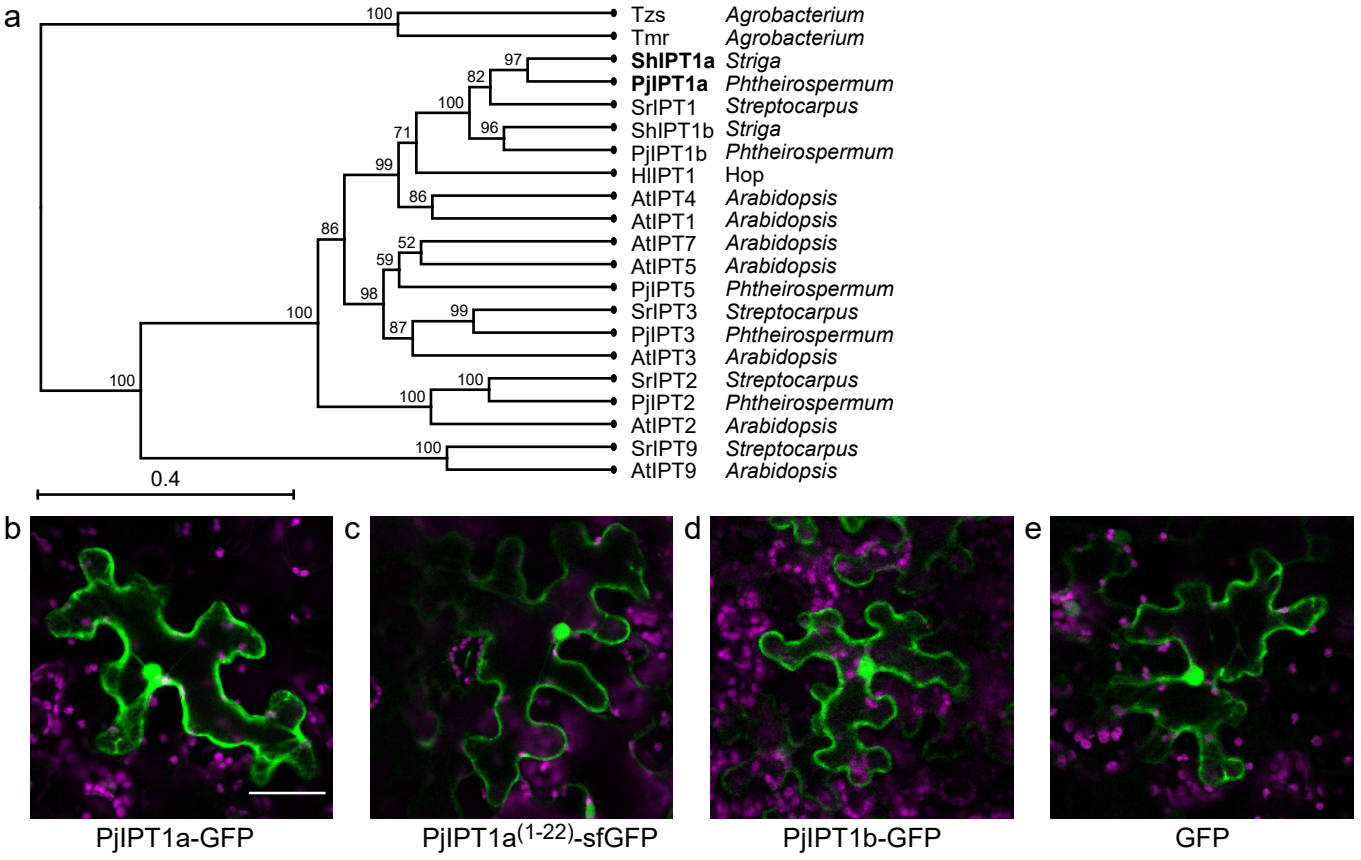
a
Tzs Agrobacterium
Tmr Agrobacterium
ShIPT1a Striga
PjIPT1a Phtheirospermum
SrIPT1 Streptocarpus
ShIPT1b Striga
PjIPT1b Phtheirospermum
HlIPT1 Hop
AtIPT4 Arabidopsis
AtIPT1 Arabidopsis
AtIPT7 Arabidopsis
AtIPT5 Arabidopsis
PjIPT5 Phtheirospermum
SrIPT3 Streptocarpus
PjIPT3 Phtheirospermum
AtIPT3 Arabidopsis
SrIPT2 Streptocarpus
PjIPT2 Phtheirospermum
AtIPT2 Arabidopsis
SrIPT9 Streptocarpus
AtIPT9 Arabidopsis
0.4
b
PjIPT1a-GFP
c
PjIPT1a(1-22)-sfGFP
d
PjIPT1b-GFP
e
GFP

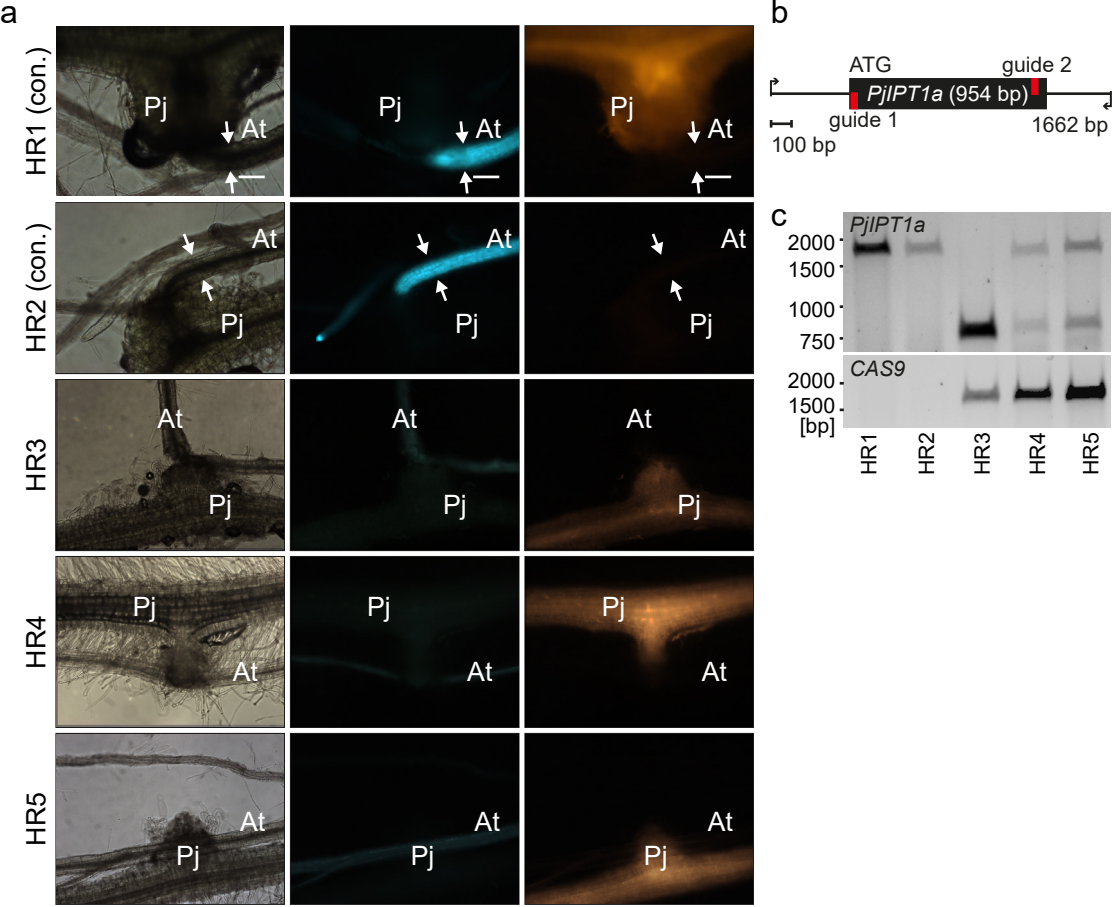

d

HR1 + HR2	GGGCCCCCATGGCGTCCACCACCACCG	AGAGGGAGGTGGTGGAACCAAGCG (Wt)
	GGGCCCCCATGGCGTCCACCACCACCG	AGAGGGAGGTGGTGGAACCAAGCG (Wt)
HR3	GGGCCCCCA----------	----------AGCG (-917)
	GGGCCCCCATGGCGTCCACCACCACCG	AGAGGGAGG-GGTGGAACCAAGCG (-1)
HR4	GGGCCCCCATGGCGTCCACCACCACCG	----------TGGAACCAAGCG (-40)
	GGGCCCCCATGGCGTCCACCA------	---------TGGTGGAACCAAGCG (-893)
	GGGCCCCCATGGCGTCCACCA------	----------(-1110)
HR5	GGGCCCCCATGGCGTCCACCAC----G	AGAGGGAG-TGGTGGAACCAAGCG (-4/-1)
	GGGCCCCCATGGCGTCCACCA------	---------TGGTGGAACCAAGCG (-894)

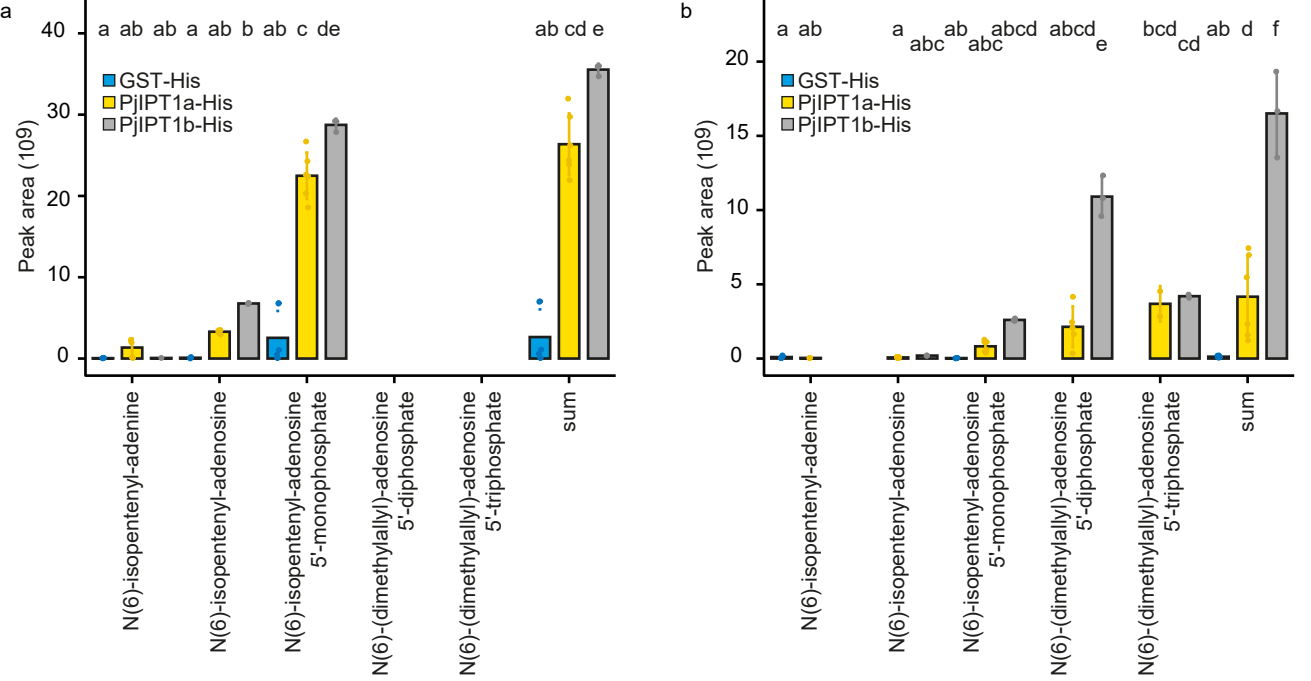
a
b
Peak area (10⁹)
GST-His
PjIPT1a-His
PjIPT1b-His
a ab ab a ab b ab c de ab cd e
a ab a abc ab abc abcd abcd e bcd cd ab d f
N(6)-isopentenyl-adenine
N(6)-isopentenyl-adenosine
N(6)-isopentenyl-adenosine 5'-monophosphate
N(6)-(dimethylallyl)-adenosine 5'-diphosphate
N(6)-(dimethylallyl)-adenosine 5'-triphosphate
sum